Design of Dye Adsorption by Amine Terminated Dendritic Functionalized Halloysite Nanotubes Using Response Surface Methodology (RSM)

Farnaz Shahamati Fard, Somaye Akbari*, Elmira Pajootan, and Mokhtar Arami

Abstract- **In this study, the adsorption performance of a modified halloysite for the removal of anionic dye (C.I. Acid Blue 92) was demonstrated. Halloysite was modified in a multistep process by the synthesis of amine terminated dendritic structures on its surface. The transmission electron microscopy images were used to characterize the nanotubes forms of pristine halloysite. The adsorption processes were performed using classical and statistical response surface methodology (RSM) techniques. The effect of important parameters such as pH, adsorbent concentration, and dye dosage was investigated. The results showed that all the independent factors except time were significant to the dye removal efficiency. The dye removal at equilibrium time was well fitted to the Langmuir isotherm model and followed the monolayer adsorption style. The adsorption rate was also described by the pseudo-second-order kinetic model. The adsorption process revealed an exothermic behavior according to the thermodynamic investigations. The removal efficiency of AB92 improved significantly from 8% to 97% after modification.**

Keywords: **halloysite, amine terminated dendritic structure, response surface methodology, removal, acid dye**

I. INTRODUCTION

Halloysite is a type of mineral clay that possesses spherical and tubular structures [1,2]. These physical structures of halloysite leads to abundance sites which can improve its adsorption efficiency for various pollutants removal. In addition to pollutant removal, halloysite has various other applications such as protective agent [3] and entrapment of active agent in controlling the rate of release [3], wound care [4], skin cleanser agent [5], composite [6-8], etc. Chemical structure of halloysite surface is divided in two classes: innermost and outermost. The Si-O bond is located onto the external curst and Al-OH linkage is settled in the internal surface [9].

Halloysite nanotubes surface has negative charge due to the containing of hydroxyl groups which makes them not appropriate for the removal of anionic pollutants like acidic dyes [10,11]. However, functionalization of halloysite can develop its application boundaries like the tendency to adsorb negatively charged contaminants [12]. The enormous specific area and lots of hydroxyl groups could also increase their modification potential [13]. One of the modification techniques is applying amine terminated groups onto the surface of halloysite [11,14]. Dendritic polymers are attractive sources of amine functional groups, which can make the halloysite positively charged to be able to remove anionic pollutants especially dye molecules [15,16].

Dyes are used in several industries such as textile, leather, printing, pharmaceutical, etc., therefore, by effluent discharge into the environment, many toxic and unsafe compounds may enter the ecosystem. Accordingly, wastewater treatment plays an important role as a damper for reducing diseases and mishap. Wastewater treatment includes different methods based on biological [17], chemical and physical processes [18]. However, adsorption has received great consideration as a promising technique because of its facile and low-cost operation.

Response surface methodology (RSM) was first introduced by G.E.P. Box and K.B. Wilson to use a first-degree polynomial equation to model the response variable in 1951 [19]. RSM is a collection of mathematical and statistical techniques that describe the experimental data obtained from the experimental design using linear or square polynomial functions. Investigation of the response variation by changing the variables and the response optimization are the main goals of using RSM. Unlike the classical design of experiment, RSM lowers the number of experiments, and the interactive effects of the studied variables are included in this method which will consequently decrease the expenses, time, reagents and materials consumption.

In the present study, amine terminated dendritic

F. Shahamati Fard, S. Akbari, E. Pajootan, and M. Arami
Department of Textile Engineering, Amirkabir University of Technology, Tehran, Iran.

Correspondence should be addressed to S. Akbari
e-mail: akbari_s@aut.ac.ir

TABLE I
STRUCTURE AND CHARACTERISTICS OF AB92

Dye	Chemical formula	W (g/mol)	Color index no.	Chemical class	Structure
AB92	$C_{26}H_{16}N_3Na_3O_{10}S_3$	695.59	13390	Diazo	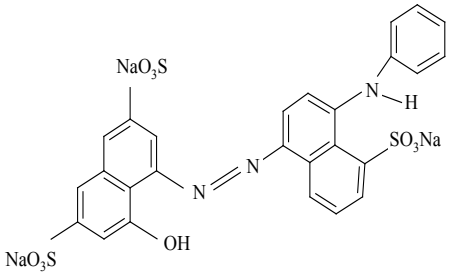

structures are applied onto the halloysite surface by a divergent synthesis method. TEM was used to study the structure of halloysite. Then, the removal condition of an anionic dye, C.I. Acid Blue 92 abbreviated by AB92, was optimized by one-variable-at-a-time and RSM using the functionalized halloysite as the adsorbent. The effect of different parameters on the adsorption performance was studied in the classical experiments and important parameters affecting the removal efficiency such as time, initial dye concentration, adsorbent dosage and pH were considered as the independent variables in RSM. The isotherm, kinetic and thermodynamic parameters of the removal process were also calculated to determine the mechanism and rate of adsorption.

II. MATERIALS AND METHODS

A. Chemicals and Materials

The halloysite powder was provided from Delta-Dolsk Company in Poland. Analytical grade Acid Blue 92 (AB92) was supplied from Ciba (Table I). Aminopropyltriethoxysilane (APTES), methyl acrylate (MA), ethanol, methanol, ethylene diamine (EDA), diethyl ether, hydrochloric acid (HCl) and all the other chemicals were obtained from Aldrich. AB92 solution was prepared with distilled water and the absorbance of solution was studied by a spectrophotometer (UNICO-2100) at 572 nm.

B. Methods

B.1. Preparation of Modified Halloysite

The preparation process of halloysite-dendritic structure (H-DS) was the result of the following strategies. Natural halloysite in contact with HCl (37%) solution was stirred for 24 h. Then, the mixture was washed several times with distilled water to remove the impurities until the pH value of the solution reached neutral and dried at 60 °C for 24 h. Amino group synthesis processes onto the halloysite were achieved by refluxing APTES in toluene at 60 °C for 12 h. The mixture was filtered and washed several times by ethanol to remove the un-reacted materials. Then, the powder was dried at 60 °C for 24 h. Michael addition of MA onto the surface of H-APTES was performed under refluxing condition. The mixture of H-APTES in methanol was refluxed by MA at 60 °C for 24 h. Finally, amine terminated groups were introduced onto the nanotube surface by refluxing condition of H-MA in methanol and EDA at 60 °C for 24 h.

The powder was washed several times with methanol and dried in an oven. The resulting product was halloysite modified by the first generation of dendritic structure (H-DSG1). For the synthesis of higher generations of dendritic structure, the last two steps were repeated till third generation. Fig. 1 represents the synthesis strategy to reach H-DSG1 [11].

B.2. Adsorption Process

The batch adsorption experiments were carried out in a 250 mL dye solution containing the desired concentration of AB92 and modified halloysite. The pH of the solution was set at 5 with HCl (0.1 N) and NaOH (0.1 N) solution. Then, the batch solution was stirred with a rate of 400 rpm on the magnetic stirrer (Heidolph, MR Hei-Standard model). At the end of adsorption experiment, the solution was centrifuged (Hettich, EBA20, Germany) for 10 min at 5000 rpm. The amounts of dye adsorbed on the adsorbent and dye removal were calculated using Eqs. (1) and (2) [20]:

$$q_t = V(C_0 - C_t)/W \tag{1}$$

$$\text{Dye Removal}(\%) = \frac{(C_0 - C_t)\times 100}{C_0} \tag{2}$$

Where, q_t is the adsorption capacity at any time (mg/g),

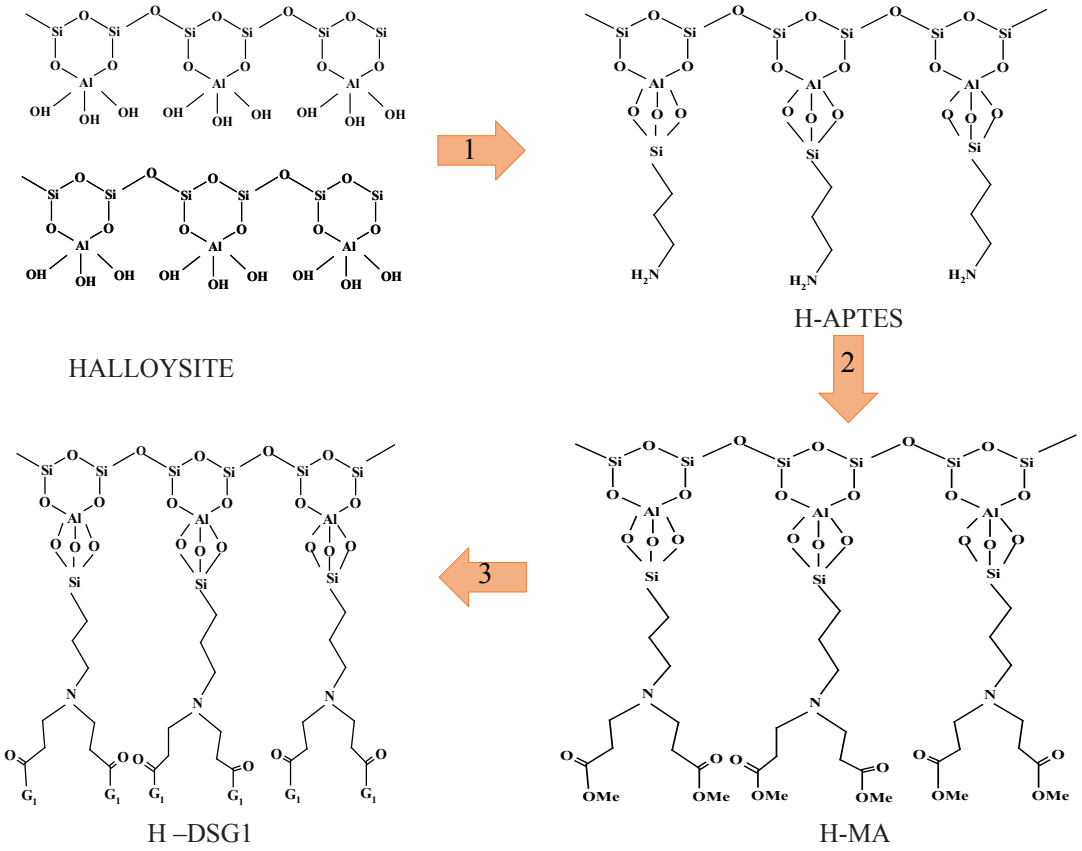

Fig. 1. Synthesis steps of amine terminated groups onto halloysite by divergent method till first generation.

C_0 and C_t are the dye concentration before and after the adsorption at various times (mg/L), V is the volume of solution (L) and W is the mass of adsorbent (g).

B.3. Characterization

The morphology of halloysite was explored using the transmission electron microscopy (TEM) model Philips CM 30.

The FTIR of HNT modified via dendrimer of third generation was obtained by Thermo-Nicolet Nexus 870 (USA).

III. RESULTS AND DISCUSSION

A. Characterization

The TEM image of pristine halloysite is represented in Fig. 2. As it is shown, raw halloysite exhibits hollow tubular structure which can facilitate the modification and efficiency of adsorption process [21,22]. The FTIR spectra of pristine halloysite and the modified halloysite of third generation are shown in Fig. 3. The corresponding functional groups assigned to each peak in the HNTs and H-DSG3 which are revealed in the spectra confirm the modification process. This is related to the dendrimer amine group located in the surface of HNTs which can be ascribed to the N-H stretching vibration groups. The peaks appeared at 2925, 2877, 1646, and 1562 cm^{-1} are attributed to the stretching vibrations of CH_2, N–H bending vibrations, and C–N bond, approving that modification of halloysite is successfully obtained.

B. Classical Optimization

B.1. Effect of Generation

The generation of the dendritic structure is one of the most important parameters determining the number of

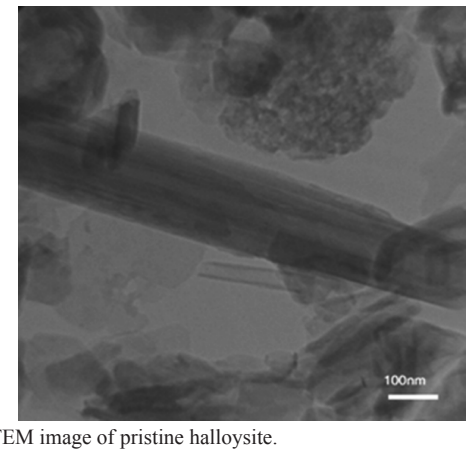

Fig. 2. TEM image of pristine halloysite.

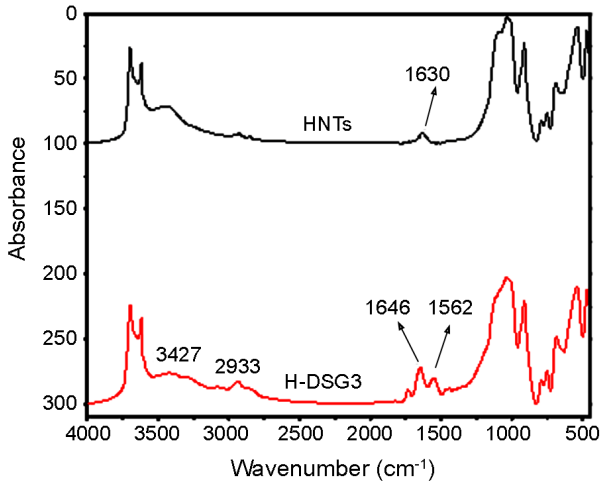

Fig. 3. FTIR spectra of pristine halloysite (HNTs) and H-DSG3.

functional groups. By growing the generation onto the halloysite, the number of amine terminated groups increase. Experiments were performed at various generations (H-DSG1, H-DSG2, and H-DSG3). The results (Fig. 4) illustrate that the amine functional groups play an important role in the removal rate. The value of dye removal was enhanced to 97% by H-DSG3 compared to the lower generations, at which H-DSG2 and H-DSG1 revealed 70 and 57% of dye removal. According to our previous study, the amine terminated groups which were induced by aminosilane coupling did not fulfill the anionic molecules adsorption containing three sulfonate groups, so higher generations of dendritic structure were synthesized on halloysite. It is worth mentioning that the evidence for chemical structure produced on the halloysite was completely investigated in our previous publish work [11].

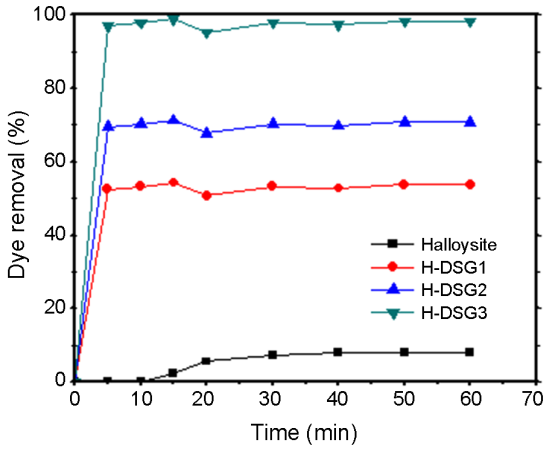

Fig. 4. Effect of generation on AB92 removal (%) by H-DSG3, H-DSG2, H-DSG1, and halloysite, (room temperature, initial dye concentration: 25 mg/L, pH: 5 and adsorbent dosage: 0.3 g/L).

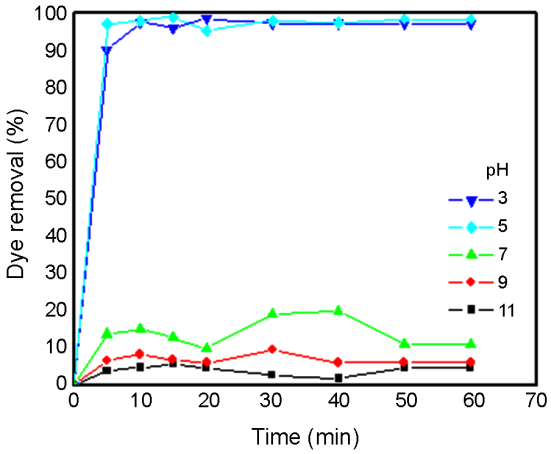

Fig. 5. Effect of pH on AB92 removal (%) by H-DSG3 (room temperature, initial dye concentration: 25 mg/L, adsorbent dosage: 0.3 g/L).

B.2. Effect of pH

As shown in Fig. 5, the effect of pH on the removal percentage of AB92 by modified halloysite is noticeable. It is clear that in acidic media (pH 3-5) the removal rate increases extraordinarily. At acidic pH, electrostatic attraction between negative and positive charges is developed sharply, which can be due to the protonation of surface amine groups in the structure of H-DS that adsorb the negative sulfonate groups located on the acidic dye. On the other hand, at higher pH values, OH^- of solution and negatively charged dye molecules compete over the adsorption sites and reduce the removal efficiency [23].

According to the experimental results, at pH 5 the removal efficiency was 97% while at higher pH values, dye removal decreased to 11%. Accordingly, the pH value of 5 was selected as the appropriate pH for AB92 adsorption.

B.3. Effect of Adsorbent Dosage

The adsorption experiments were investigated in a

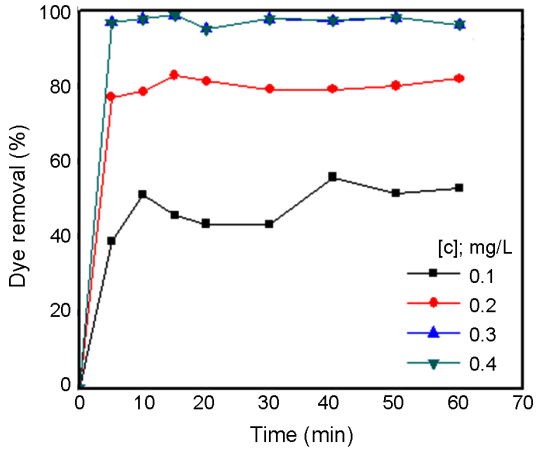

Fig. 6. Effect of adsorbent dosage on AB92 removal (%) by H-DSG3, (room temperature, initial dye concentration: 25 mg/L, pH: 3).

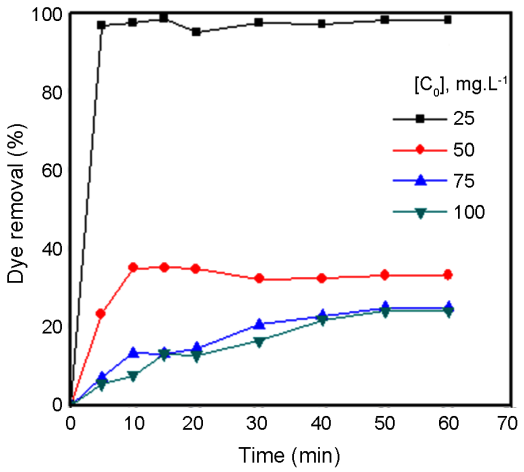

Fig. 7. Effect of initial dye concentration on AB92 removal (%) by H-DSG3 (room temperature, pH: 5, adsorbent dosage: 0.3 g/L).

particular range of sorbent dosage (0.1 g/L to 0.4 g/L). Fig. 6 illustrates the effect of adsorbent dosage on the removal efficiency. It can be seen that the dye removal efficiency increases from 53% to 97% by the addition of higher dosages of adsorbent. The optimum dosage was chosen 0.3 g/L, because at higher adsorbent dosages the probability of agglomeration increases which results in lower specific surface area of adsorbent [24].

B.4. Effect of Initial Dye Concentration

As it can be seen in Fig. 7, the dye removal decreased significantly by increasing the dye concentration. Effect of initial dye concentration on the adsorption was examined from 25 mg/L to 100 mg/L at room temperature, pH 5 and optimum sorbent dosage (0.3 g/L). Experimental results show 97% removal for 25 mg/L of AB92, while the results at the same condition represent 24% of dye removal for 100 mg/L of dye solution. This decrease in the efficiency is probably due to the insufficient adsorption sites to remove higher concentrations of dye [25].

B.5. Effect of Temperature

Fig. 8 reveals that the adsorption of AB92 decreased by increasing the temperature from 298 K to 328 K. This phenomenon was related to the increasing competition between dye molecules for settling onto the adsorption sites which were located on the surface of H-DS. The equilibrium adsorption capacity was obviously affected by increasing the temperature and changed from 82.3 mg/g at 298 K to 49.8 mg/g at 328 K. The experimental results represented that the adsorption onto the H-DS was more favorable at lower temperatures [26,27].

C. Adsorption Isotherms

Adsorption isotherm is known as an important factor which explains the mechanism of adsorption and the reactions occurring between the adsorbent and adsorbate. The Langmuir, Temkin and Freundlich isotherms were investigated which are represented in Eqs. (3) to (5), respectively.

$$\frac{C_e}{q_e} = \frac{1}{K_L Q_m} + \frac{C_e}{Q_m} \tag{3}$$

$$q_e = B \ln K_T + B \ln C_e \tag{4}$$

$$\log q_e = \log K_F + \frac{1}{n} \log C_e \tag{5}$$

Where, C_e is the concentration of AB92 at equilibrium (mg/L) and q_e is the amount of dye adsorbed per unit mass of sorbent (mg/g). Q_m is the maximum amount of adsorption capacity (mg/g), K_L is the Langmuir equilibrium constant (L/mg), B=RT/b, T is the absolute temperature (K), R is the gas constant (8.314 J/K.mol), and K_F and 1/n are constant

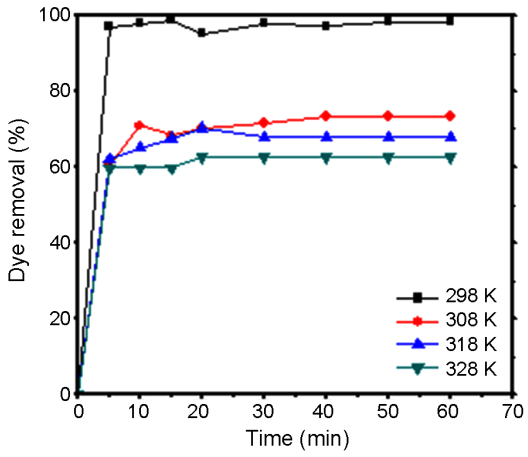

Fig. 8. Effect of temperature on AB92 removal (%) by H-DSG3 (initial dye concentration: 25 mg/L, pH: 5, adsorbent dosage: 0.3 g/L).

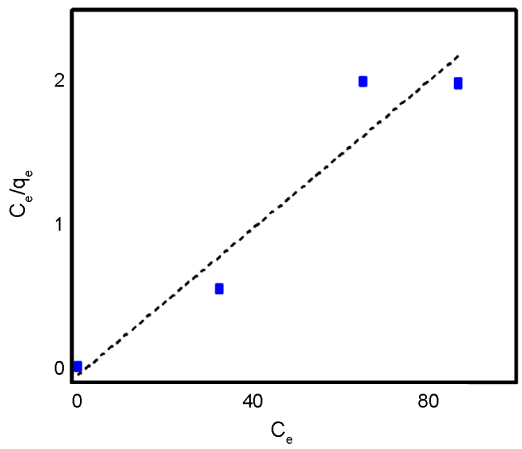

Fig. 9. Langmuir isotherm of AB92 onto H-DSG3 at different initial dye concentrations.

TABLE II
ISOTHERM PARAMETERS FOR THE ADSORPTION OF AB92 ONTO H-DSG3

Dye	Langmuir				Temkin			Freundlich		
	Q_m	K_L	R_L	R^2	B_1	K_T	R^2	K_F	N	R^2
AB92	81.89	0.47	0.04-0.02	0.92	-0.733	0.0003	0.83	71.9	-7.9	0.72

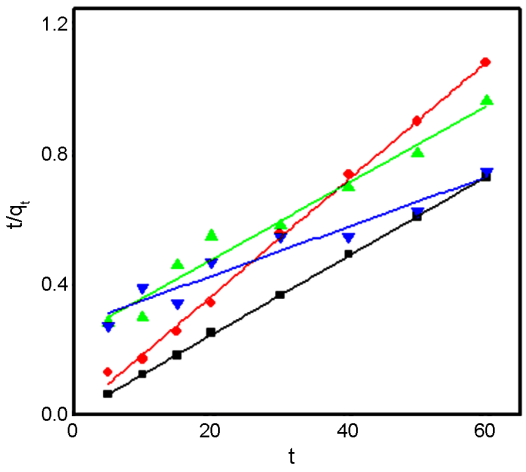

Fig. 10. Pseudo-second-order adsorption kinetic of AB92 onto H-DSG3 at different initial dye concentrations.

values, where K_F illustrates the adsorption capacity and 1/n is related to the adsorption strength [28].

Table II also represents all associated parameters of isotherms and according to the R^2 values, the adsorption isotherm of AB92 followed the Langmuir isotherm model (Fig. 9) which illustrates the monolayer adsorption of AB92 onto the H-DSG3. On the other hand, all adsorption sites possess equal energy without any coverage with other adsorbed molecules onto the adsorbent sites. Although, there are lots of branched in dendritic structure onto the H-DSG3, strong electrostatic force is needed to overcome the dendritic boxes in de Gennes dense packed. As a results, the isotherm confirms the monolayer adsorption of AB92 onto the H-DSG3.

The additional factor explaining the adsorption reversibility in Langmuir model is defined as R_L. The process is irreversible when R_L is 0; favorable when R_L is between 0 and 1, linear when R_L is 1, and unfavorable when R_L is higher than 1. R_L is written as Eq. (6) [28,29]:

$$R_L = \frac{1}{1 + K_L C_0} \tag{6}$$

The results in Table II indicate that the adsorption process is favorable for AB92 on H-DSG3.

D. Adsorption Kinetics

Kinetic of adsorption is studied as an important factor to determine the rate of adsorption. According to Fig. 10 it can be obtained that the rate of adsorption follows the pseudo-second-order model. In addition, pseudo-first-order and intra particle models were also investigated, but as Table III shows, adsorption did not follow these models. The values of the correlation coefficients (R^2) in the range of 0.83 to 0.99 demonstrated that pseudo-second-order is the fitted kinetic model.

TABLE III
KINETIC PARAMETERS FOR THE ADSORPTION OF AB92 ONTO H-DSG3

		Pseudo-first-order				Pseudo-second-order			Intraparticle diffusion		
Dye	C_0 (mg/L)	q_e (mg/g)	$q_e(c)$ (mg/g)	k_1 (1/min)	R^2	q_e (mg/g)	k_2 (g/mg.min)	R^2	c (mg/g)	k_{dif} (mg/g.min$^{1/2}$)	R^2
AB92	25	82.3	5.5	0.04	0.39	81.96	0.099	0.99	38.5	7.5	0.47
	50	58.5	4.38	0.01	0.02	55.2	0.0003	0.99	22.8	5.6	0.53
	75	32.5	5.7	0.04	0.39	73.2	0.0001	0.92	1.14	8.4	0.97
	100	43.6	14.3	0.06	0.57	104.1	0.0004	0.83	-4.3	11.3	0.97

TABLE IV
THERMODYNAMIC PARAMETERS OF AB92 ADSORPTION ON H-DSG3

Dye	q_e (mg/g)	T (K)	ΔG^0 (kJ/mol)	ΔH^0 (kJ/mol)	ΔS^0 (kJ/mol.K)
AB92	83.3	298	-14011.1	-101089.9	-300.21
	56.86	308	-5040.7		
	56.2	318	-5118.1		
	49.86	328	-4333.83		

The linear forms of pseudo-second-order, pseudo-first-order and intra particle models are represented in Eqs. (7) to (9):

$$\log(q_e - q_t) = \log(q_e) - \frac{k_1}{2.303t} \quad (7)$$

$$\frac{t}{q_t} = \frac{1}{k_2 q_e^2} + \left(\frac{1}{q_e}\right)t \quad (8)$$

$$q_t = K_{dif} t^{\frac{1}{2}} + C \quad (9)$$

Where, q_e and q_t (mg/g) are the amount of dye adsorbed at equilibrium and time t (min), respectively, and k_1 (1/min) is the pseudo-first-order rate constant, k_2 is the pseudo-second-order rate constant (g/mg.min), K_{dif} is the intraparticle diffusion rate constant (mg/g.min$^{1/2}$) and C is the intercept (mg/g) which explains the width of the layers [30,31].

E. Adsorption Thermodynamics

In order to study the thermodynamic behavior of adsorption, some parameters such as ΔG^0(kJ/mol), ΔH^0(kJ/mol), and ΔS^0(kJ/mol.K) are considered. In this regard, experiments were performed at various ranges of temperature (298-328 K). The Van't Hoff plot of Ab92 adsorption onto H-DSG3 is illustrated in Fig. 11. Table IV shows the negative values of ΔG^0, ΔH^0, and ΔS^0 which indicate a spontaneous exothermic adsorption process with decreasing randomness at the interface of adsorbent/adsorbate. These parameters were

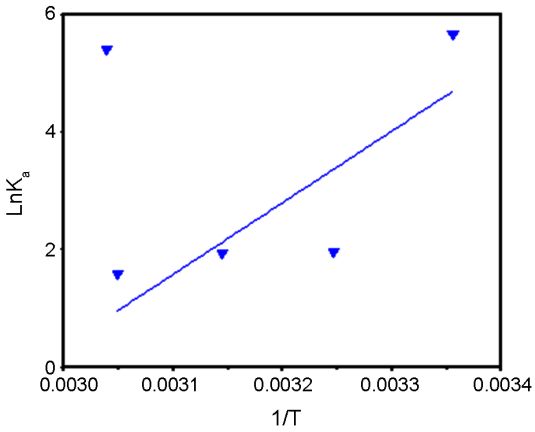

Fig. 11. Van't Hoff plot of Ab92 onto H-DSG3.

calculated according to the Eqs. (10) and (11) as below:

$$\ln K_L = \frac{\Delta S^0}{R} - \frac{\Delta H^0}{RT} \quad (10)$$

$$\Delta G^0 = \Delta H^0 - T\Delta S^0 \quad (11)$$

Where, K_L is the Langmuir constant, R is the universal gas constant, and T is the absolute temperature (K) [26].

F. RSM Optimization

31 experimental runs were performed according to the central composite design (CCD) with 6 repetitive experiments at the central point. The independent variables and their values which were selected in accordance with the

TABLE V
PARAMETERS AND THEIR SCOPES IN CENTRAL COMPOSITE DESIGN

Parameter	Factors	Unit	Scope				
			2	1	0	-1	-2
Time	X_1	min	25	20	15	10	5
pH	X_2	-	6	5	4	3	2
Adsorbent dosage	X_3	g/L	0.6	0.5	0.4	0.3	0.2
Dye concentration	X_4	mg/L	45	40	35	30	25

TABLE VI
RESULTS OF CCD EXPERIMENTS

Test	Time (X_1)	pH (X_2)	Adsorbent dosage (X_3)	Initial conc. (X_4)	Dye removal (%)	
					Experimental	Predicted
1	20	5	0.5	40	80.08	70.74
2	10	5	0.3	40	41.11	34.10
3	20	3	0.5	30	99.11	104.8
4	20	5	0.3	30	51.46	54.5
5	10	3	0.5	30	97.97	103.38
6	5	4	0.4	35	97.95	96.88
7	10	5	0.5	40	63.67	61.8
8	15	4	0.4	35	98.33	98.33
9	20	5	0.3	40	41.86	36.98
10	15	4	0.4	35	98.33	98.33
11	15	2	0.4	35	98.10	90.40
12	15	4	0.4	35	98.33	98.33
13	15	4	0.4	35	98.33	90.40
14	15	4	0.2	35	69.42	98.33
15	15	4	0.4	35	98.33	98.33
16	15	4	0.6	35	99.30	67.68
17	10	3	0.3	30	94.96	98.33
18	10	3	0.5	40	98.38	101.75
19	15	4	0.4	25	99.14	103.06
20	25	4	0.4	35	99.48	94.04
21	15	4	0.4	35	98.33	85.17
22	20	3	0.3	40	82.67	101.27
23	20	5	0.5	30	72.80	98.33
24	10	3	0.3	40	85.27	82.02
25	20	3	0.3	30	96.19	72.21
26	10	5	0.3	30	51.24	84.87
27	20	3	0.5	40	98.85	98.51
28	15	4	0.4	35	98.33	53.37
29	15	6	0.4	35	5.79	97.25
30	15	4	0.4	45	43.59	98.33
31	20	5	0.5	30	78.54	14.2

results from classical experiments are reported in Table V. The results of adsorption experiments according to CCD are reported in the Table VI. The analysis of variance (ANOVA, Table VII), normality, regression analysis, and lack of fit test can be employed to examine the adequacy of model for the removal of AB92.

The values of correlation coefficients indicate how well the estimated model fits the data. It is shown in Fig. 12 that the normal probability of residuals for AB92 dye are approximately along a straight line, which means that the normality assumption of response is satisfied.

The main effect of each parameter on dye removal using 0.4 g/L of adsorbent at pH 4 for 15 min is represented in Fig. 13. According to this figure, adsorbent dosage had an increasing effect, while pH and dye concentration had decreasing effect on the response function in the specified range.

The three dimensional response plots of removal efficiency against two variables are shown in Fig. 14. It can be seen that increasing the time of adsorption did

TABLE VII
ANOVA FOR AB92 ADSORPTION

Source	Degree of freedom	Sum of square	Mean square	F	P
Regression	14	1607.3	1207.66	21.75	0.000
Linear	4	11656.4	2891.34	52.07	0.000
Square	4	4846.5	1211.6	21.82	0.000
Intercept	6	495.4	82.572	1.49	0.245
Residual	16	888.5	55.53		
Lack of fit	10	888.5	88.85	*	*
Error	6	0	0		
Total	30	11795.8	-	-	-

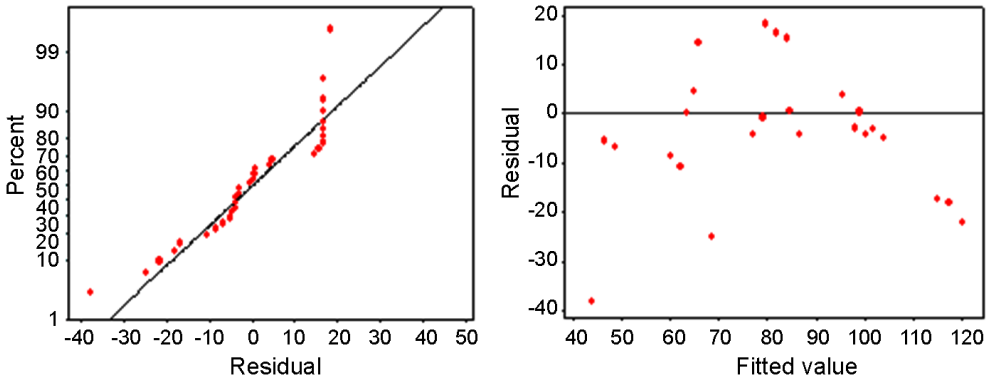

Fig. 12. Normal probability and residual plots of AB92.

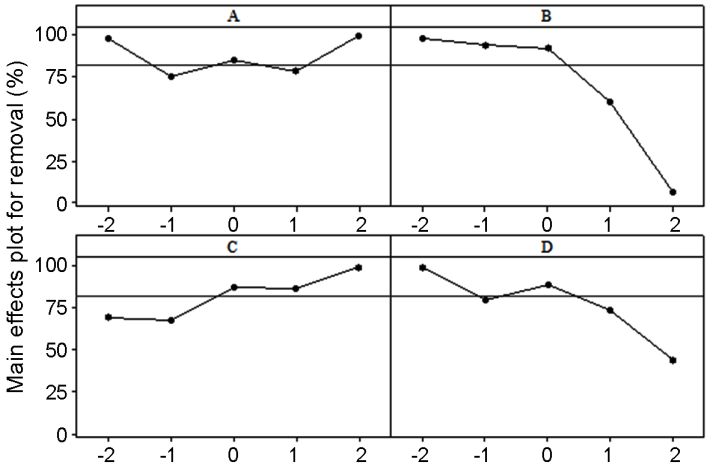

Fig. 13. Main effect of each parameter on dye removal: (A) time, (B) pH, (C) adsorbent dosage, and (D) dye concentration.

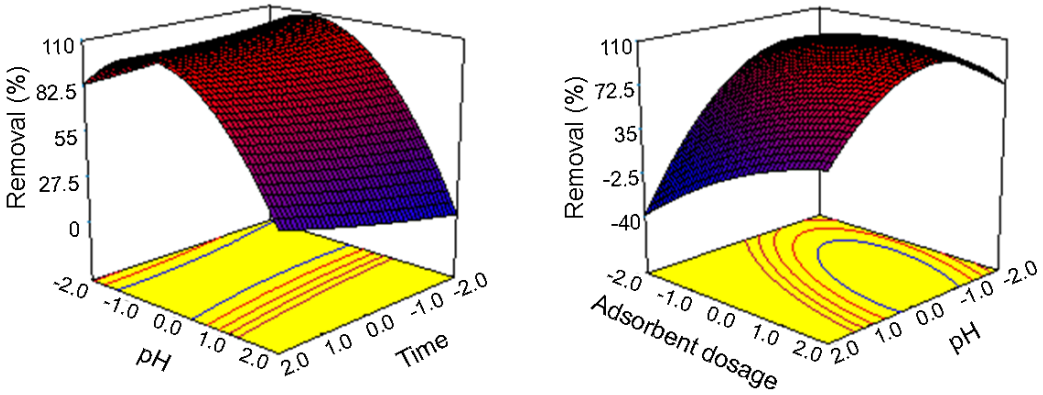

Fig. 14. 3D surface plots of AB92.

not affect the removal (%) of AB92 significantly as it was demonstrated by its high P-value (P>0.5) due to the existence of three sulfonate groups in its structure. The presence of high number of sulfonate groups in the structure of AB92 may increase the rate of adsorption and lower the equilibrium time. Fig. 13 also indicates that by increasing the adsorbent dosage from 0.2 g/L to 0.6 g/L and decreasing the pH value, the AB92 removal (%) increases due to the availability of more adsorption sites and the availability of positive amine functional groups at low pH values.

IV. CONCLUSION

The adsorption of Acid Blue 92 as an acidic model dye with three sulfonate groups (AB92) onto the pristine and modified halloysite with amine terminated dendritic structures has been investigated in this present work. Transmission electron microscopy (TEM) image showed the tubular shape of halloysite. The effect of pH, initial dye concentration, sorbent dosage and temperature were studied in the classical experiments, and the experimental results showed that the modified halloysite exhibited high adsorption capacity at 15 min (equilibrium time) and the removal efficiency of AB92 improved significantly from 8% to 97% after the synthesis of generation 3 amine functionalized dendritic structure. Response surface methodology (RSM) was employed as a statistical method to investigate the adsorption of AB92 onto the modified halloysite. The P-values and ANOVA indicated that all the independent factors except for time were significant to the response function (dye removal efficiency) and confirmed the validity and accuracy of the model. The study of equilibrium parameters demonstrated that the dye removal was well fitted to the Langmuir isotherm model. The kinetic of adsorption followed the pseudo-second-order model. Furthermore, the thermodynamic study revealed an exothermic and spontaneous adsorption with decreasing randomness at the surface of the modified halloysite.

REFERENCES

[1] A.F. Peixoto, A.C. Fernandes, C. Pereira, J. Pires, and C. Freire, "Physicochemical characterization of organosilylated halloysite clay nanotubes", *Micropor. Mesopor. Mater.*, vol. 219, pp. 145-154, 2016.

[2] Y.M. Chen, L. Yu, and X.W.D. Lou, "Hierarchical tubular structures composed of Co_3O_4 hollow nanoparticles and carbon nanotubes for lithium storage", *Angew. Chem., Int. Ed.,* doi:10.1002/ange.201600133.

[3] Y.M. Lvov, D.G. Shchukin, H. Mohwald, and R.R. Price, "Halloysite clay nanotubes for controlled release of protective agents", *ACS Nano*, vol. 2, pp. 814-820, 2008.

[4] G. Cavallaro, "Innovative smart materials designed for environmental purposes", ph.D dissertation, University of Palermo, Sicily, 2013.

[5] M.T. Dodd, D.A. Jakubovic, C.D. Putman, M.R. Sine, C.P. Thomas, and K.S. Wei, "Skin sanitizing compositions", EP1152743A1, 2001.

[6] C.K. Choo, X.Y. Kong, T.L. Goh, G.C. Ngoh, B.A. Horri, and B. Salamatinia, "Chitosan/halloysite beads fabricated by ultrasonic-assisted extrusion-dripping and a case study application for copper ion removal", *Carbohyd. Polym*., vol. 138, pp. 16-26, 2016.

[7] D. Papoulis, D. Panagiotaras, P. Tsigrou, K. Christoforidis, C. Petit, A. Apostolopoulou et al., "Halloysite and sepiolite-TiO_2 nanocomposites: synthesis characterization and photocatalytic activity in three aquatic wastes", *Mat. Sci. Semicon. Proc.,* vol. 85, pp. 1-8, 2018.

[8] D. Papoulis, "Halloysite based nanocomposites and

photocatalysis: a review", *Appl. Clay Sci.*, vol. 168, pp. 164-174, 2019.

[9] E. Joussein, S. Petit, J. Churchman, B. Theng, D. Righi, and B. Delvaux, "Halloysite clay minerals-a review", *Clay Miner.*, vol. 40, pp. 383-426, 2005.

[10] C. Chao, J. Liu, J. Wang, Y. Zhang, B. Zhang, Y. Zhang et al., "Surface modification of halloysite nanotubes with dopamine for enzyme immobilization", *ACS Appl. Mater. Inter.*, vol. 5, pp. 10559-10564, 2013.

[11] F. Shahamati Fard, S. Akbari, E. Pajootan, and M. Arami, "Enhanced acidic dye adsorption onto the dendrimer-based modified halloysite nanotubes", *Desalin. Water Treat.*, vol. 57, no. 54, pp. 1-18, 2016.

[12] S. Rooj, A. Das, V. Thakur, R. Mahaling, A.K. Bhowmick, and G. Heinrich, "Preparation and properties of natural nanocomposites based on natural rubber and naturally occurring halloysite nanotubes", *Mater. Design*, vol. 31, pp. 2151-2156, 2010.

[13] R. Kamble, M. Ghag, S. Gaikawad, and B.K. Panda, "Halloysite nanotubes and applications: a review", *J. Adv. Sci. Res.*, vol. 3, no. 2, pp. 25-29, 2012.

[14] S. Cataldo, G. Lazzara, M. Massaro, N. Muratore, A. Pettignano, and S. Riela, "Functionalized halloysite nanotubes for enhanced removal of lead (II) ions from aqueous solutions", *Appl. Clay Sci.*, vol. 156, pp. 87-95, 2018.

[15] J. Zhang, D. Zhang, A. Zhang, Z. Jia, and D. Jia, "Dendritic polyamidoamine-grafted halloysite nanotubes for fabricating toughened epoxy composites", *Iran. Polym. J.,* vol. 22, pp. 501-510, 2013.

[16] B. Theng, M. Russell, G. Churchman, and R. Parfitt, "Surface properties of allophane, halloysite, and imogolite", *Clay. Clay Miner.*, vol. 30, pp. 143-149, 1982.

[17] C.L. Grady Jr, G.T. Daigger, N.G. Love, and C.D. Filipe, *Biological Wastewater Treatment:* CRC Press, 2011.

[18] E. Riser-Roberts, *Remediation of Petroleum Contaminated Soils: Biological, Physical, and Chemical Processes: CRC Press*, 1998.

[19] M.A. Bezerra, R.E. Santelli, E.P. Oliveira, L.S. Villar, and L.A. Escaleira, "Response surface methodology (RSM) as a tool for optimization in analytical chemistry", *Talanta*, vol. 76, pp. 965-977, 2008.

[20] B. Noroozi, G. Sorial, H. Bahrami, and M. Arami, "Equilibrium and kinetic adsorption study of a cationic dye by a natural adsorbent-silkworm pupa", *J. Hazard. Mater.*, vol. 139, pp. 167-174, 2007.

[21] N.G. Veerabadran, R.R. Price, and Y.M. Lvov, "Clay nanotubes for encapsulation and sustained release of drugs", *Nano*, vol. 2, pp. 115-120, 2007.

[22] S. Levis and P. Deasy, "Characterisation of halloysite for use as a microtubular drug delivery system", *Int. J. Pharm.*, vol. 243, pp. 125-134, 2002.

[23] L. Liu, Y. Wan, Y. Xie, R. Zhai, B. Zhang, and J. Liu, "The removal of dye from aqueous solution using alginate-halloysite nanotube beads", *Chem. Eng. J.*, vol. 187, pp. 210-216, 2012.

[24] M. Bhaumik, R.I. McCrindle, A. Maity, S. Agarwal, and V.K. Gupta, "Polyaniline nanofibers as highly effective re-usable adsorbent for removal of reactive black 5 from aqueous solutions", *J. Colloid Interface Sci*., vol. 466, pp. 442-451, 2016.

[25] T. Anirudhan and M. Ramachandran, "Adsorptive removal of basic dyes from aqueous solutions by surfactant modified bentonite clay (organoclay): Kinetic and competitive adsorption isotherm", *Process Saf. Environ.*, vol. 95, pp. 215-225, 2015.

[26] J. Fu, Z. Chen, M. Wang, S. Liu, J. Zhang, J. Zhang et al., "Adsorption of methylene blue by a high-efficiency adsorbent (polydopamine microspheres): kinetics, isotherm, thermodynamics and mechanism analysis", *Chem. Eng. J.*, vol. 259, pp. 53-61, 2015.

[27] D.A. Giannakoudakis, G.Z. Kyzas, A. Avranas, and N.K. Lazaridis, "Multi-parametric adsorption effects of the reactive dye removal with commercial activated carbons", *J. Mol. Liq.*, vol. 213, pp. 381-389, 2016.

[28] F. Gomri, M. Boutahala, H. Zaghouane-Boudiaf, S.A. Korili, and A. Gil, "Removal of acid blue 80 from aqueous solutions by adsorption on chemical modified bentonites", *Desalin. Water Treat.*, pp. 1-10, 2016.

[29] T. Madrakian, A. Afkhami, and M. Ahmadi, "Adsorption and kinetic studies of seven different organic dyes onto magnetite nanoparticles loaded tea waste and removal of them from wastewater samples", *Spectrochim. Acta A: Mol. Biomol. Spectrosc.*, vol. 99, pp. 102-109, 2012.

[30] M. Viseras, C. Aguzzi, P. Cerezo, C. Viseras, and C. Valenzuela, "Equilibrium and kinetics of 5-aminosalicylic acid adsorption by halloysite", *Micropor. Mesopor. Mat.*, vol. 108, pp. 112-116, 2008.

[31] R. Liu, B. Zhang, D. Mei, H. Zhang, and J. Liu, "Adsorption of methyl violet from aqueous solution by halloysite nanotubes", *Desalination*, vol. 268, pp. 111-116, 2011.